Open access • Journal Article • DOI:10.1148/RADIOL.2482071307

Functionally Relevant Coronary Artery Disease : Comparison of 64-Section CT Angiography with Myocardial Perfusion SPECT — Source link

Oliver Gaemperli, Tiziano Schepis, Ines Valenta, Pascal Koepfli ...+7 more authors

Institutions: University of Zurich

Published on: 01 Aug 2008 - Radiology (Radiological Society of North America)

Topics: Angiography, Myocardial perfusion imaging, Perfusion scanning, Coronary artery disease and Coronary arteries

Functionally relevant coronary artery disease: comparison of 64-section CT angiography with myocardial perfusion SPECT

Gaemperli, O; Schepis, T; Valenta, I; Koepfli, P; Husmann, L; Scheffel, H; Leschka, S; Eberli, F R; Luscher, T F; Alkadhi, H; Kaufmann, P A

Functionally relevant coronary artery disease: comparison of 64-section CT angiography with myocardial perfusion SPECT

Abstract

PURPOSE: To prospectively determine the accuracy of 64-section computed tomographic (CT) angiography for the depiction of coronary artery disease (CAD) that induces perfusion defects at myocardial perfusion imaging with single photon emission computed tomography (SPECT), by using myocardial perfusion imaging as the reference standard. MATERIALS AND METHODS: All patients gave written informed consent after the study details, including radiation exposure, were explained. The study protocol was approved by the local institutional review board. In patients referred for elective conventional coronary angiography, an additional 64-section CT angiography study and a myocardial perfusion imaging study (1-day adenosine stress-rest protocol) with technetium 99m-tetrofosmin SPECT were performed before conventional angiography. Coronary artery diameter narrowing of 50% or greater at CT angiography was defined as stenosis and was compared with the myocardial perfusion imaging findings. Quantitative coronary angiography served as a reference standard for CT angiography. RESULTS: A total of 1093 coronary segments in 310 coronary arteries in 78 patients (mean age, 65 years +/- 9 [standard deviation]; 35 women) were analyzed. CT angiography revealed stenoses in 137 segments (13%) corresponding to 91 arteries (29%) in 46 patients (59%). SPECT revealed 14 reversible, 13 fixed, and six partially reversible defects in 31 patients (40%). Sensitivity, specificity, and negative and positive predictive values, respectively, of CT angiography in the detection of reversible myocardial perfusion imaging defects were 95%, 53%, 94%, and 58% on a per-patient basis and 95%, 75%, 96%, and 72% on a per-artery basis. Agreement between CT and conventional angiography was very good (96% and kappa = 0.92 for patient-based analysis, 93% and kappa = 0.84 for vessel-based analysis). CONCLUSION: Sixty-four-section CT angiography can help rule out hemodynamically relevant CAD in patients with intermediate to high pretest likelihood, although an abnormal CT angiography study is a poor predictor of ischemia.

Functionally Relevant Coronary Artery Disease: Comparison of 64-Section CT Angiography with Myocardial Perfusion SPECT[1]

Oliver Gaemperli, MD
Tiziano Schepis, MD
Ines Valenta, MD
Pascal Koepfli, MD
Lars Husmann, MD
Hans Scheffel, MD
Sebastian Leschka, MD
Franz R. Eberli, MD
Thomas F. Luscher, MD
Hatem Alkadhi, MD
Philipp A. Kaufmann, MD

Purpose: To prospectively determine the accuracy of 64-section computed tomographic (CT) angiography for the depiction of coronary artery disease (CAD) that induces perfusion defects at myocardial perfusion imaging with single photon emission computed tomography (SPECT), by using myocardial perfusion imaging as the reference standard.

Materials and Methods: All patients gave written informed consent after the study details, including radiation exposure, were explained. The study protocol was approved by the local institutional review board. In patients referred for elective conventional coronary angiography, an additional 64-section CT angiography study and a myocardial perfusion imaging study (1-day adenosine stress-rest protocol) with technetium 99m–tetrofosmin SPECT were performed before conventional angiography. Coronary artery diameter narrowing of 50% or greater at CT angiography was defined as stenosis and was compared with the myocardial perfusion imaging findings. Quantitative coronary angiography served as a reference standard for CT angiography.

Results: A total of 1093 coronary segments in 310 coronary arteries in 78 patients (mean age, 65 years ± 9 [standard deviation]; 35 women) were analyzed. CT angiography revealed stenoses in 137 segments (13%) corresponding to 91 arteries (29%) in 46 patients (59%). SPECT revealed 14 reversible, 13 fixed, and six partially reversible defects in 31 patients (40%). Sensitivity, specificity, and negative and positive predictive values, respectively, of CT angiography in the detection of reversible myocardial perfusion imaging defects were 95%, 53%, 94%, and 58% on a per-patient basis and 95%, 75%, 96%, and 72% on a per-artery basis. Agreement between CT and conventional angiography was very good (96% and $\kappa = 0.92$ for patient-based analysis, 93% and $\kappa = 0.84$ for vessel-based analysis).

Conclusion: Sixty-four–section CT angiography can help rule out hemodynamically relevant CAD in patients with intermediate to high pretest likelihood, although an abnormal CT angiography study is a poor predictor of ischemia.

[1] From the Cardiovascular Center (O.G., T.S., I.V., P.K., F.R.E., T.F.L., P.A.K.) and Institute of Diagnostic Radiology (L.H., H.S., S.L., H.A.), University Hospital Zurich, Ramistrasse 100, NUK C 32, CH-8091 Zurich, Switzerland; and the Zurich Center for Integrative Human Physiology, University of Zurich, Switzerland (P.A.K.). Received July 24, 2007; revision requested September 10; revision received October 27; accepted December 14; final version accepted January 7, 2008. Supported by a grant from the Swiss National Science Foundation (professorship grant no. PP00A-68835) and by a grant of the National Center of Competence in Research, Computer Aided and Image Guided Medical Interventions of the Swiss National Science Foundation. **Address correspondence to** P.A.K. (e-mail: *pak@usz.ch*).

The latest refinements in computed tomographic (CT) technology, including faster gantry rotations, multidetector arrays, and dual-source devices, have advanced CT angiography as a promising alternative to conventional coronary angiography for the diagnosis of coronary artery disease (CAD) in selected groups of patients (1,2). Recent studies comparing 64-section CT angiography with conventional angiography (3–8) have documented high sensitivity (73%–100%) and specificity (90%–97%) for CT angiography in the detection of coronary artery stenoses. The diagnostic accuracy has resulted in the implementation of CT angiography as an alternative diagnostic technique in symptomatic patients who have inconclusive findings at stress electrocardiography (ECG) or who are unable to exercise (1,2). Nevertheless, CT angiography still has important limitations, such as motion artifacts and heavy calcifications, that might prevent accurate and reliable morphologic evaluation (3). Furthermore, the morphologic quality inherent in all angiographic images—such as CT and conventional angiograms—does not allow assessment of the hemodynamic relevance of a given coronary lesion (9,10).

Myocardial perfusion imaging with single photon emission computed tomography (SPECT) is a widely established method for noninvasively evaluating the hemodynamic significance of coronary artery stenoses (11). In addition to its diagnostic accuracy, SPECT provides important prognostic information that may be helpful for cardiac risk stratification and in guiding further therapeutic decisions (12–14). By contrast, the purely anatomic information depicted with invasive and noninvasive angiographic techniques offers limited hemodynamic and prognostic data on which clinical decision-making can be based (9), unless additional techniques such as fractional flow reserve measurements or intravascular ultrasonography are applied.

Recent reports of studies in small groups of patients (15–18) indicate that CT angiography is an accurate tool for ruling out hemodynamically relevant CAD but that it has only limited value for the detection of lesions that induce perfusion defects at myocardial perfusion imaging. However, these studies included relatively small numbers of patients, used 16-section CT, or did not include conventional angiography for the validation of CT angiography results. Thus, the purpose of our study was to prospectively determine the accuracy of 64-section CT angiography in the depiction of CAD that induces perfusion defects at myocardial perfusion imaging with SPECT, by using myocardial perfusion imaging as the reference standard.

Advances in Knowledge

- In our moderately large-scale study, 64-section CT angiography had a excellent negative predictive value (94%–96%) for the detection of coronary stenoses associated with myocardial ischemia at SPECT.
- Like conventional coronary angiography, CT angiography had a low positive predictive value (58%–72%) for the diagnosis of hemodynamically relevant coronary artery disease (CAD) (ie, coronary lesions with perfusion defects at myocardial perfusion imaging).

Materials and Methods

Patients

Patients known to have or suspected of having CAD who were referred to our institution for elective conventional angiography were asked to undergo myocardial perfusion imaging and CT angiography (in that sequence) prior to the invasive procedure. Reasons for referral were typical or atypical chest pain, pathologic exercise test results, or dyspnea. Patients were eligible if they were in stable clinical condition—that is, if they had Canadian Cardiovascular Society class I–III and New York Heart Association functional class I–III cardiovascular disease. Exclusion criteria were severe obstructive lung disease, high-grade atrioventricular conduction disturbances, atrial fibrillation, and known intolerance of iodinated contrast agents. The patients' clinical characteristics were obtained from a short clinical history and a cardiovascular examination performed prior to imaging by an experienced physician with at least 2 years of experience in clinical cardiology (O.G., T.S., I.V., or P.A.K.). The study protocol was approved by the institutional review board of the University Hospital Zurich, the ethics committee of the Canton of Zurich, and the national radiation safety committee, and all patients gave written informed consent before enrollment. Written informed consent was ob-

Implication for Patient Care

- Our findings suggest that CT angiography is an excellent noninvasive alternative imaging technique to conventional coronary angiography for ruling out hemodynamically relevant CAD in patients with an intermediate to high pretest likelihood.

Published online before print
10.1148/radiol.2482071307

Radiology 2008; 248:414–423

Abbreviations:
AUC = area under the ROC curve
CAD = coronary artery disease
CI = confidence interval
ECG = electrocardiography
LAD = left anterior descending
LCX = left circumflex
NPV = negative predictive value
PPV = positive predictive value
RCA = right coronary artery
ROC = receiver operating characteristic

Author contributions:
Guarantors of integrity of entire study, O.G., P.A.K.; study concepts/study design or data acquisition or data analysis/interpretation, all authors; manuscript drafting or manuscript revision for important intellectual content, all authors; manuscript final version approval, all authors; literature research, O.G., T.S., I.V., P.K., L.H., H.S., S.L., H.A., P.A.K.; clinical studies, O.G., T.S., I.V., P.K., H.S., S.L., F.R.E., T.F.L., H.A., P.A.K.; statistical analysis, O.G., L.H., H.A., P.A.K.; and manuscript editing, all authors

Authors stated no financial relationship to disclose.

tained from all the patients after all the details of the study, including information on radiation exposure, were explained. Design and conduct of the study were based on the recommendations issued by the Standards for Reporting of Diagnostic Accuracy steering group (19).

CT Angiogram Acquisition

All examinations were performed with a 64-section CT scanner (Somatom Sensation 64; Siemens Medical Solutions, Forchheim, Germany). Scanning parameters were as follows: detector collimation, 32 × 0.6 mm; section collimation, 64 × 0.6 mm by means of a z-flying focal spot; gantry rotation time, 330 msec; pitch, 0.2; tube voltage, 120 kV; and tube current–time product, 700 mAs. A bolus of 80 mL of iodixanol (Visipaque 320 [320 mg of iodine per milliliter]; GE Healthcare, Buckinghamshire, England) followed by 30 mL of saline solution was continuously injected into a right antecubital vein through an 18-gauge catheter at a flow rate of 5 mL/sec. Bolus tracking was performed with a region of interest (size range, one-quarter to one-third of the diameter of the ascending aorta) placed in the ascending aorta by an experienced radiographer (L.H., H.S., or S.L., each with at least 2 years of experience in cardiovascular imaging), and image acquisition was automatically started 5 seconds after the signal attenuation reached the predefined threshold of 140 HU.

Synchronized to the ECG data, CT data sets were retrospectively reconstructed in 5% steps from 30% to 80% of the R-R interval. The "adaptive cardio volume" approach was used for image reconstruction. This approach switches to a two-segment reconstruction algorithm at heart rates greater than 65 beats per minute. ECG pulsing for radiation dose reduction was used in all patients. All patients were in stable sinus rhythm, and the mean heart rate during the CT examination was 62 beats per minute ± 9 (standard deviation). All patients received 1.25–2.5 mg of sublingual isosorbiddinitrate (Isoket Spray; Schwarz Pharma, Munchenstein, Switzerland) 2–3 minutes before CT angiography, and 10 patients were pretreated with 5–15 mg of intravenous metoprolol tartrate (Lopresor; Daiichi Sankyo, Thalwil, Switzerland). No serious adverse events secondary to nitroglycerin, metoprolol, or contrast agent administration were reported.

All data sets were reconstructed by using a medium soft-tissue convolution kernel (B30f) with an effective section thickness of 1 mm and increments of 0.8 mm (mean field of view, 155 mm ± 21; range, 120–175 mm; image matrix, 512 × 512 pixels). The data set that provided the best image quality was reconstructed with the same parameters by using a sharp tissue convolution kernel (B46f). All data were transferred to an external workstation (Leonardo; Siemens).

CT Angiogram Interpretation

CT angiogram interpretation was performed with axial source images, multiplanar and curved reformations, and thin-slab maximum intensity projections. First, image quality for each data set was rated by one reader (L.H., with 3 years of experience in cardiovascular imaging) by using a previously published five-point ranking scale (20): a score of 1 indicated no motion artifacts and clear delineation of the segment; a score of 2, minor artifacts and mild blurring of the segment; a score of 3, moderate artifacts and moderate blurring without structure discontinuity; a score of 4, severe artifacts and doubling or discontinuity in the course of the segment; and a score of 5, that the image was nonevaluable and vessel structures were not differentiable. Coronary arteries were subdivided ac-

Figure 1

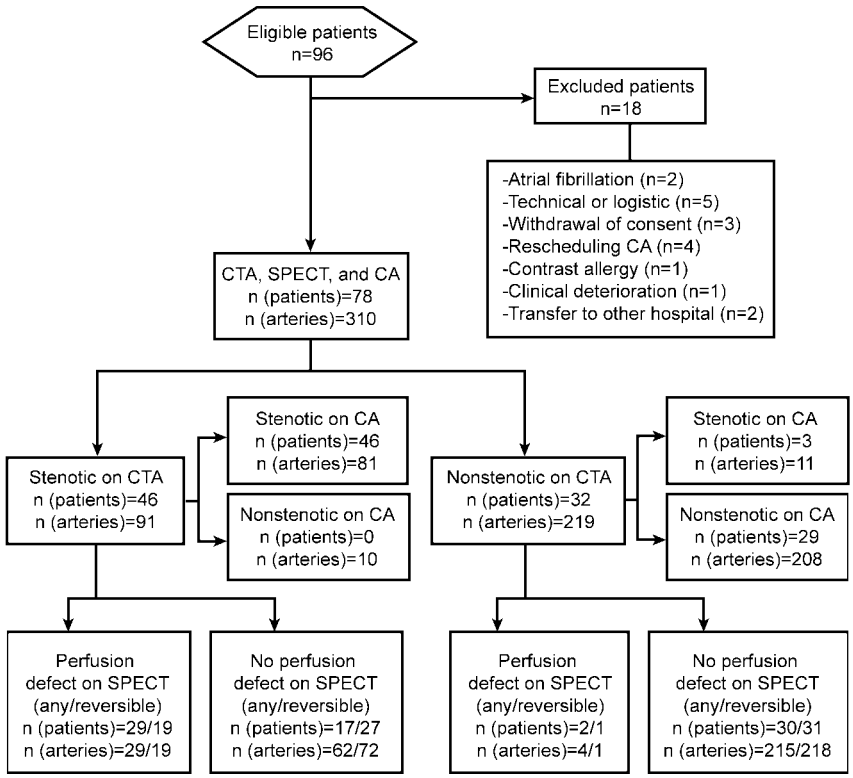

Figure 1: Flowchart of study participants. (SPECT results are displayed as any perfusion defect *[any]* or as reversible perfusion defects only *[reversible]*.) Of note, a patient is categorized as having CAD (ie, *stenotic* and *perfusion defect*) if at least one lesion is present. Because multiple lesions may be present in a single patient, the numbers of lesions cannot be calculated from the patient-based analysis but must be individually identified. *CA* = coronary angiography, *CTA* = 64-section CT angiography.

cording to a 15-segment model proposed by the American Heart Association (21).

Then, each segment was visually evaluated in two planes—one parallel and one perpendicular to the course of the vessel—with regard to coronary artery delineation. On these images, the degree of diameter stenosis was semiquantitatively graded on a decimal scale in 10% steps from 0% to 100% by two independent radiologists (L.H. and H.A., with 5 years of experience) who were both blinded to the clinical history and to the findings from myocardial perfusion imaging and conventional angiography. In cases of disagreement in stenosis grading of greater than 10%, a consensus reading between both readers was performed. When the difference between readers was 10%, the mean diameter stenosis was calculated. A significant stenosis was defined as narrowing of the coronary diameter of 50% or greater, and all vessels with a diameter of 1.5 mm or greater were included in the analysis.

Myocardial Perfusion Imaging Image Acquisition

SPECT imaging was performed by using a 1-day ECG-gated stress-rest protocol. Pharmacologic stress was induced by infusion of adenosine (0.33% solution in 0.9% saline, created by local university pharmacy division) at a standard rate of 140 μg per kilogram of body weight per minute (22), and a dose of 250–350 MBq of technetium 99m–tetrofosmin was injected 3 minutes into the state of pharmacologic stress. This was followed by an injection of three times the stress dose at rest according to a standard protocol (23). Patients were told to refrain from ingesting caffeine-containing beverages for at least 12 hours, nitrates and calcium channel blockers for 24 hours, and β-blockers for 48 hours before the myocardial perfusion imaging study. Gated SPECT studies were performed with a dual-head detector camera (Millenium VG & Hawkeye; GE Healthcare); a low-energy, high-resolution collimator; a 20% symmetric window at 140 keV; a 64 × 64 matrix; an elliptic orbit with step-and-shoot acquisition at 3° intervals over 180°; and a 20-second dwell time per stop. Acquisitions were gated at 16 frames per R-R cycle with a 50% window of acceptance.

For all patients, the summed nongated SPECT image set was reconstructed at a dedicated workstation (eNTEGRA or Xeleris; GE Medical Systems, Milwaukee, Wis) by using an iterative reconstruction algorithm (ordered-subset expectation maximization with two iterations and 10 subsets) with x-ray based attenuation correction as previously described (24,25) into short-axis, vertical long-axis, and horizontal long-axis sections encompassing the entire left ventricle. In addition, polar maps of perfusion, wall motion, and wall thickening were produced by using a commercially available software package (Cedars QGS/QPS; Cedars-Sinai Medical Center, Los Angeles, Calif) (26). No serious adverse events following radionuclide injection or pharmacologic stress agent administration were reported. Image quality of myocardial perfusion images was amenable to visual interpretation in all patients.

Myocardial Perfusion Image Interpretation

SPECT image interpretation was visually performed in consensus by two nu-

Table 1

Clinical Characteristics in 78 Patients

Characteristic	Datum
Age (y)*	65 ± 9
No. of women	35 (45)
Body mass index (kg/m^2)*	26 ± 4
Systolic blood pressure (mm Hg)*	134 ± 19
Diastolic blood pressure (mm Hg)*	78 ± 12
Cardiovascular history	
No known CAD	59 (76)
Known CAD	19 (24)
Single-vessel CAD	5 (6)
Two-vessel CAD	5 (6)
Three-vessel CAD	9 (12)
Previous myocardial infarction and/or acute coronary syndrome	16 (21)
Previous percutaneous coronary intervention	19 (24)
Previous coronary artery bypass graft	1 (1)
Pathologic exercise test result	35 (45)
Left ventricular ejection fraction (%)*†	59 ± 15
Symptoms	
Canadian Cardiovascular Society class I–III angina pectoris	30 (38)
Atypical chest pain	16 (21)
New York Heart Association class I–III dyspnea	29 (37)
None	13 (17)
Cardiovascular risk factors	
Diabetes mellitus	13 (17)
Hypertension	61 (78)
Dyslipidemia	40 (51)
Current or former smoker	40 (51)
Current medication	
Aspirin	70 (90)
Angiotensin converting enzyme inhibitor and/or angiotensin II receptor blocker	41 (53)
β-Receptor antagonist	47 (60)
Statin	32 (41)
Calcium channel blocker	7 (9)

Note.—Unless otherwise indicated, data are numbers of patients, with percentages in parentheses.

* Data are means ± standard deviations.

† As assessed with gated SPECT.

clear cardiologists (O.G., with 3 years of experience in cardiac radionuclide imaging, and P.A.K., with 10 years of experience)—both of whom were blinded to the clinical history and to the findings from CT and conventional angiography—on short-axis, horizontal long-axis, and vertical long-axis sections and semiquantitative polar maps of perfusion as previously reported (27). Anterior and septal wall perfusion defects were allocated to the left anterior descending (LAD) coronary artery, lateral defects were allocated to the left circumflex (LCX) coronary artery, and inferior defects were allocated to the right coronary artery (RCA). In the watershed regions, allocation was determined according to the main extension of the defect onto the lateral, anterior, or inferior wall. Reversible perfusion defects were considered to represent myocardial ischemia. Fixed perfusion defects with concomitant regional wall motion abnormalities were considered to be myocardial scars (27). A partially reversible defect was defined as a fixed defect that increased in size during stress.

Figure 2

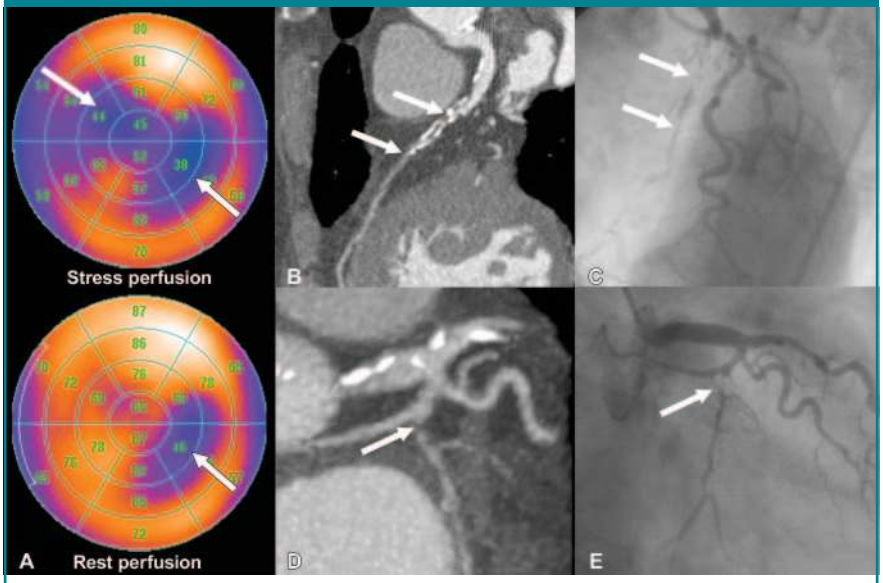

Figure 2: Images in 60-year-old woman referred for ischemic chest pain. *A,* Myocardial perfusion SPECT polar maps reveal a reversible septal defect (left arrow) and a partially reversible inferolateral defect (right arrows). *B,* Multiplanar curved reformation of CT angiography data shows diffuse disease and high-grade stenoses in the proximal and middle LAD artery (arrows) that were confirmed at, *C,* conventional coronary angiography. *D,* Maximum intensity projection of CT angiography data reveals a high-grade stenosis of the ostial LCX artery (arrow) that was also confirmed at, *E,* conventional angiography.

Quantitative Coronary Angiography

Conventional coronary angiography was performed according to standard techniques, and multiple views were digitally stored on a designated workstation. The angiograms were evaluated by an experienced observer (F.R.E., with 15 years of experience in invasive coronary angiography) who was blinded to the results from CT angiography and myocardial perfusion imaging. The coronary arteries were subdivided according to the same model used for the CT angiography images (21) and were quantitatively assessed with the use of an automated edge-detection system (Xcelera 1.2; Philips Medical Systems, Best, the Netherlands). Quantitative coronary angiography measurements were performed (for all lesions visually estimated to represent narrowing greater than 25%) in two image planes and included the diameter of the reference vessel (proximal and distal to the stenosis), the minimal luminal diameter, and the extent of stenosis (defined as the diameter of the reference vessel minus the minimal luminal diameter, divided by the reference diameter and multiplied by 100%). For biplane assessment, diameters obtained in both image planes were averaged. A significant stenosis was defined as a diameter reduction of 50% or greater.

Statistical Analysis and Reference Standards

To evaluate the diagnostic performance of CT angiography in the detection of coronary stenoses that induced perfusion defects at myocardial perfusion imaging (reference standard), we performed a patient-based and a vessel-based analysis. Sensitivity, specificity, and accuracy were calculated from χ^2 tests of contingency, and 95% confidence intervals (CIs) were calculated from binomial expression. Accuracy was determined as the percentage of correct diagnoses in the entire sample (28). Nonevaluable segments were censored as positive findings in the vessel-based and patient-based analyses, reflecting the intention-to-diagnose nature of the study (29). We calculated negative predictive values (NPVs) and positive predictive values (PPVs) by incorporating disease prevalence on the basis of the Bayes formula and likelihood ratios for a positive or negative test result as previously reported (30). The CT angiography results were further compared with the findings from quantitative coronary angiography, the latter being the reference standard for the diagnosis of coronary artery stenoses.

Agreement between CT and conventional angiography was assessed with Cohen κ statistics. Univariate logistic regression analysis was used to compare the findings from CT angiography and conventional angiography with the myocardial perfusion imaging results. The regression results are presented as odds ratios and their respective 95% CIs. Receiver operating characteristic (ROC) analysis was applied to compare the diagnostic performance of CT angiography and conventional angiography (using the cutoff for significant coronary stenoses as the variable parameter) in the detection of reversible

perfusion defects by comparing the respective areas under the ROC curve (AUCs) (28). The optimal cutoff point was determined by using the Youden index (*J* value) (calculated as the maximum of $J = SN + SP - 1$, where SN is sensitivity and SP is specificity, for each cutoff value) (31).

Figure 3

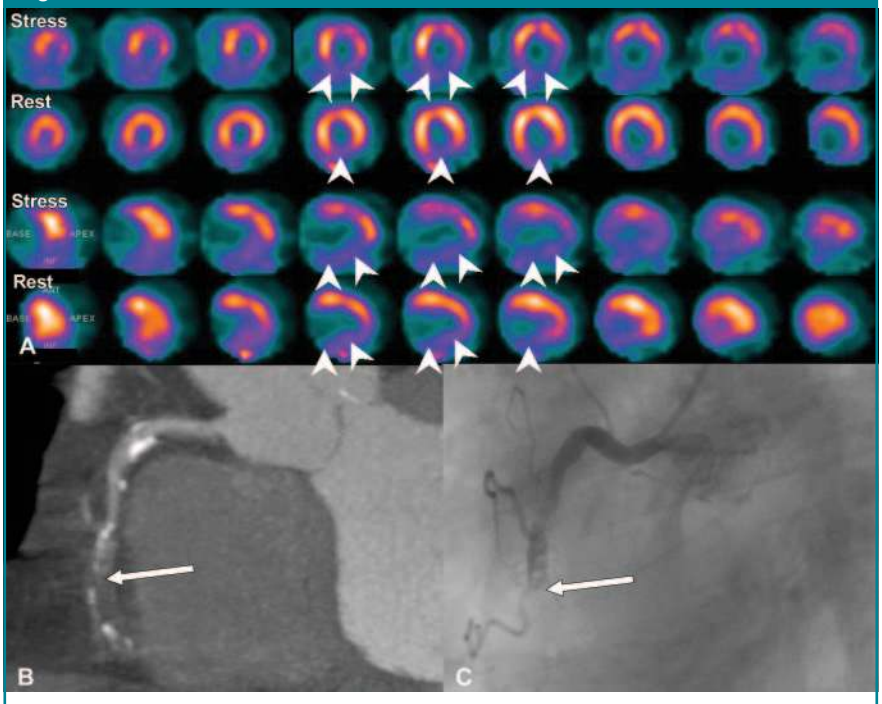

Figure 3: Images in 68-year-old man referred for evaluation of ischemic chest pain. *A*, Myocardial perfusion SPECT short-axis (upper two rows) and vertical long-axis sections (lower two rows) show a partially reversible large inferior perfusion defect (arrowheads). *B*, Multiplanar reconstruction in the RCA at CT angiography shows a complete occlusion in its midportion (arrow) that was confirmed at, *C*, conventional coronary angiography.

Figure 4

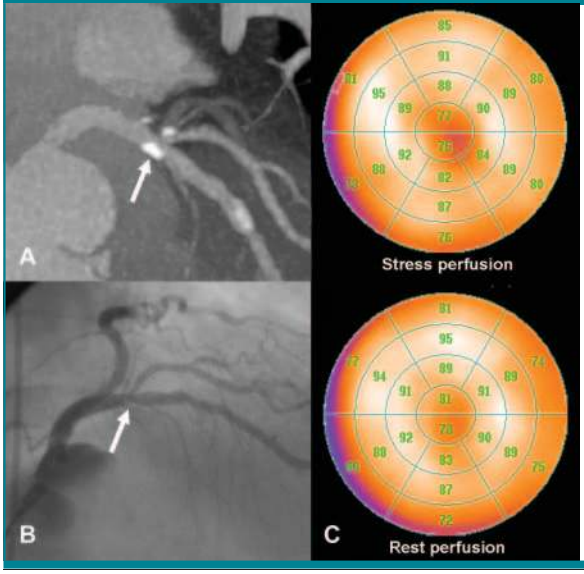

Figure 4: Example images in 58-year-old man indicate disagreement between CT angiography and SPECT. *A*, Maximum intensity projection of CT angiography data shows calcified plaque of the proximal LAD artery with an estimated stenosis of 60% (arrow). *B*, At conventional coronary angiography, stenosis appears to be less than 50% (arrow) (37% at quantitative coronary angiography), which suggests overestimation at CT angiography because of partial volume effects originating from the calcifications. *C*, Stress-rest SPECT perfusion polar maps show normal perfusion.

Statistical analysis was performed by using software (SPSS, version 12.0.1 for Windows; SPSS, Chicago, Ill). Quantitative data are expressed as means ± standard deviations, and categoric data are given as percentages. A two-tailed *P* value of less than .05 was considered to indicate a statistically significant difference for all tests.

Results

Ninety-six patients were enrolled in our study. Seven patients did not undergo CT angiography because of atrial fibrillation ($n = 2$) or technical or logistic reasons ($n = 5$). Eleven patients did not undergo conventional angiography because of withdrawal of consent ($n = 3$), rescheduling of conventional angiography because of patient inconvenience ($n = 4$), contrast agent allergy ($n = 1$), rapid deterioration of clinical condition ($n = 1$), or transfer to another hospital ($n = 2$). The remaining 78 patients were included in our analysis (Fig 1). The mean age was 65 years ± 9 (range, 40–87 years), and 35 patients (45%) were women (Table 1). Nineteen patients (24%) had known CAD. The remaining 59 patients (76%) had a mean 10-year Framingham risk score for cardiovascular events of 12 ± 9. The median time interval between CT angiography and myocardial perfusion imaging was 0 days (range, 0–26 days), that between CT angiography and conventional angiography was 1 day (range, 0–22 days), and that between myocardial perfusion imaging and conventional angiography was 1 day (range, 0–26 days). All CT angiography and myocardial perfusion imaging studies were performed prior to the conventional angiography procedure.

CT Angiography

A total of 1093 coronary segments in 310 main coronary arteries were analyzed. In two patients, the left main artery was missing as the LAD and LCX arteries had separate origins from the left coronary sinus. The mean calcium score was 668 Agatston units ± 858. Eight (1%) coronary segments in five

Table 2

Accuracy of 64-Section CT Angiography for Detection of Perfusion Defects at Myocardial Perfusion Imaging

Analysis	Sensitivity (%)*	Specificity (%)*	NPV (%)	PPV (%)	Accuracy (%)*	Positive Likelihood Ratio	Negative Likelihood Ratio
Patient-based analysis ($n = 78$)							
Any perfusion defect†	94 (79, 99)	64 (49, 77)	94	63	76 (65, 85)	2.59	0.10
Reversible perfusion defects only	95 (75, 100)	53 (40, 67)	94	58	64 (52, 75)	2.04	0.09
Coronary artery–based analysis ($n = 310$)							
Any perfusion defect†	88 (72, 97)	78 (72, 82)	91	72	79 (74, 83)	3.93	0.16
Reversible perfusion defects only	95 (75, 100)	75 (70, 80)	96	72	76 (71, 81)	3.83	0.07

* Data in parentheses are 95% CIs expressed as percentages.

† Including fixed, reversible, and mixed defects.

patients were nonevaluable because of insufficient image quality (score, 5) due to motion artifacts or heavy calcifications; these segments were therefore considered to be stenosed in an intention-to-diagnose–based approach. Including these segments, visual CT angiography image analysis revealed a stenosis in 137 (13%) of 1093 segments corresponding to 91 (29%) of 310 coronary arteries (left main artery, $n = 0$; LAD artery, $n = 33$; LCX artery, $n = 28$; RCA, $n = 30$) in 46 (59%) of 78 patients (Fig 1).

Myocardial Perfusion Imaging

Visual image analysis revealed 14 reversible, 13 fixed, and six partially reversible perfusion defects in 31 (40%) of 78 patients. The distribution of the perfusion defects among the different coronary artery territories was as follows: Reversible perfusion defects were found in the LAD artery ($n = 8$), LCX artery ($n = 2$), and RCA ($n = 4$), and fixed perfusion defects were found in the LAD artery ($n = 4$), LCX artery ($n = 3$), and RCA ($n = 6$), while partially reversible perfusion defects were found in the LAD artery ($n = 1$), LCX artery ($n = 1$), and RCA ($n = 4$).

Comparison of 64-Section CT Angiography with Conventional Coronary Angiography

Overall CAD prevalence at conventional angiography (defined by the presence of at least one stenosed coronary segment per patient) was 63% (49 of 78). Of the 92 coronary arteries with stenoses at conventional angiography, 81 were correctly identified with CT angiography (Figs 2, 3), whereas 11 were underestimated and therefore misclassified with CT angiography. Conversely, of the 218 nonstenotic coronary arteries, 208 were correctly identified at CT angiography, while 10 were erroneously classified as stenotic (Fig 4). Sensitivity, specificity, NPV, PPV, and accuracy, respectively, of CT angiography in the detection of coronary stenoses seen at conventional angiography (assuming a disease prevalence of 63% at conventional angiography) were 94% (46 of 49; 95% CI: 83%, 99%), 100% (29 of 29; 95% CI: 88%, 100%), 91%, 100%, and 96% (75 of 78; 95% CI: 89%, 99%) at patient-based analysis and 88% (81 of 92; 95% CI: 80%, 94%), 95% (208 of 218; 95% CI: 92%, 98%), 82%, 97%, and 93% (289 of 310; 95% CI: 90%, 96%) at vessel-based analysis. Overall agreement between CT angiography and conventional angiography for the detection of coronary stenoses was 96% (75 of 78; 95% CI: 89%, 99%; $\kappa = 0.92$) at patient-based analysis and 93% (289 of 310; 95% CI: 90%, 96%; $\kappa = 0.84$) at vessel-based analysis.

Vessel- and Patient-based Comparison of 64-Section CT Angiography versus Myocardial Perfusion Imaging

Of the 91 coronary arteries (in 46 patients) with significant stenoses at CT angiography, 29 were associated with a perfusion defect at myocardial perfusion imaging (Figs 1–3); the perfusion defect was purely reversible in 19 of these 29 coronary arteries. The remaining 62 stenosed coronary arteries were not associated with any perfusion defect at myocardial perfusion imaging (Fig 4). On the other hand, of the 219 arteries (in 32 patients) without any coronary stenoses at CT angiography, only four had a perfusion defect at myocardial perfusion imaging. The defect was purely reversible in one of these four arteries. At patient-based analysis, the resulting sensitivity, specificity, NPV, PPV, and accuracy, respectively, of 64-section CT angiography for the detection of hemodynamically relevant coronary artery lesions (assuming a myocardial perfusion imaging disease prevalence of 40%) were 94% (29 of 31), 64% (30 of 47), 94%, 63%, and 76% (59 of 78) for any perfusion defect and 95% (19 of 20), 53% (31 of 58), 94%, 58%, and 64% (50 of 78) for purely reversible perfusion defects (Table 2). At vessel-based analysis, sensitivity, specificity, NPV, PPV, and accuracy, respectively, of 64-section CT angiography for the detection of hemodynamically relevant coronary artery lesions were 88% (29 of 33), 78% (215 of 277), 91%, 72%, and 79% (244 of 310) for any perfusion defect and 95% (19 of 20), 75% (218 of 290), 96%, 72%, and 76% (237 of 310) for purely reversible perfusion defects (Table 2). At patient-based analysis, the positive likelihood ratios were 2.59 and 2.04 and the negative likelihood ratios were 0.10 and 0.09 for any perfusion defect and purely reversible perfusion defects, respectively. At vessel-based analysis, the positive likelihood ratios were 3.93 and 3.83 and the negative likelihood ratios were 0.16 and 0.07 for any per-

fusion defect and for purely reversible perfusion defects, respectively (Table 2).

Stenosis Severity and Related Perfusion Defect

Logistic regression analysis revealed a positive correlation between the percentage degree of stenosis at quantitative coronary angiography and the presence of any perfusion defect (odds ratio, 1.03; 95% CI: 1.02, 1.05; $P < .001$) or reversible perfusion defects only (odds ratio, 1.05; 95% CI: 1.03, 1.07; $P < .001$). A similar correlation was present for stenoses at CT angiography and any perfusion defects (odds ratio, 1.05; 95% CI: 1.03, 1.06; $P < .001$) or reversible perfusion defects only (odds ratio, 1.06; 95% CI: 1.03, 1.08; $P < .001$). On the basis of logistic regression analysis equations, the projected probability of ischemia was similar for any given degree of diameter stenosis at quantitative coronary angiography versus that at CT angiography (Fig 5). ROC analysis showed a similar diagnostic performance of CT angiography compared with quantitative coronary angiography for the detection of reversible perfusion defects (AUC, 0.88 [95% CI: 0.80, 0.96] vs AUC, 0.87 [95% CI: 0.79, 0.94]; $P > .05$) (Fig 6). The optimal lesion severity cutoff for predicting ischemia was 58% or greater at quantitative coronary angiography and 60% or greater at CT angiography. With these cutoff values, sensitivity, specificity, positive likelihood ratio, and negative likelihood ratio, respectively, for the detection of coronary stenosis that induced myocardial ischemia at SPECT were 94% (95% CI: 70%, 99%), 72% (95% CI: 65%, 79%), 3.38, and 0.09 for quantitative coronary angiography and 94% (95% CI: 70%, 99%), 73% (95% CI: 66%, 80%), 3.46, and 0.09 for CT angiography.

Figure 5

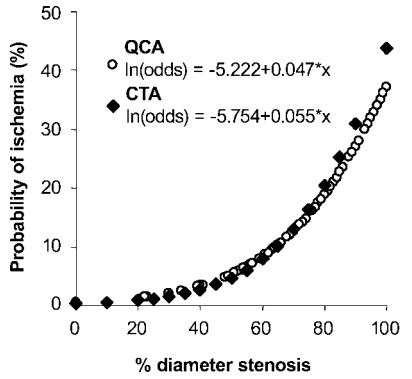

Figure 5: Exponential probability curves derived from logistic regression analysis equations (insert) show predicted probability of ischemia (as assessed with SPECT) for any given degree of stenosis at quantitative coronary angiography *(QCA)* versus CT angiography *(CTA)*.

Discussion

The results of our study indicate that 64-section CT angiography has excellent abilities in ruling out hemodynamically relevant CAD, as indicated by the high NPV in this intermediate-to-high–risk population. Conversely, an abnormal 64-section CT angiography study is a poor predictor of ischemia, and further myocardial perfusion imaging testing is warranted in these patients to identify those who might benefit from a revascularization procedure (14) and those in whom conservative management and risk modification may be justified.

Figure 6

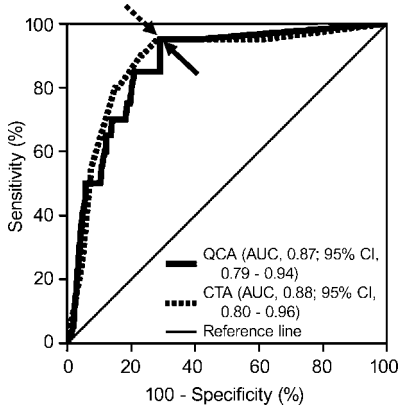

Figure 6: ROC curves for comparison of diagnostic performance of quantitative coronary angiography *(QCA)* and CT angiography *(CTA)* in the detection of purely reversible perfusion defects at myocardial perfusion imaging. The AUC is similar for CT angiography and quantitative coronary angiography in both graphs ($P > .05$ for both comparisons). The optimal cutoffs for coronary stenoses associated with myocardial ischemia are calculated at 58% or greater for quantitative coronary angiography (solid arrow) and 60% or greater for CT angiography (dotted arrow).

Our results are in line with those of previous studies with 16-section and 64-section CT angiography (15–18). Hacker et al (15,16) reported a high NPV in ruling out hemodynamically relevant CAD with both scanner types and a low PPV with the 16-section CT scanner (29%) and the 64-section device (53%) (15,16). These results were confirmed by Schuijf and colleagues (17), who showed that only 59% of coronary stenoses 50% or greater at CT angiography were associated with a perfusion defect at SPECT. Predictive values were similar (NPV, 99%; PPV, 50%) in a previously published study by Gaemperli et al (18). However, several features of the latter studies need to be mentioned: First, the number of study participants was limited, rendering particularly a patient-based analysis difficult. Second, conventional coronary angiography results were not available in all patients. Third, no attenuation correction was performed for the SPECT images. And finally, a relatively large number of study participants were excluded because of insufficient image quality (15,16). Our study was designed to overcome these shortcomings by including a higher number of subjects, by ensuring that conventional coronary angiography was performed in all patients, by enhancing the diagnostic accuracy of SPECT by using x-ray–based attenuation correction, and, finally, by performing data interpretation on an intention-to-diagnose basis by censoring nonevaluable coronary arteries or patients as positive findings.

There are several explanations for the modest performance of 64-section CT angiography in the prediction of hemodynamically relevant CAD. For example, CT angiography results tend to overestimate coronary stenoses, particularly if calcifications are present, as compared with conventional coronary angiography (3–7). Furthermore, a false-negative CT angiography finding may result from a SPECT finding that is erroneously interpreted as a perfu-

sion defect (ie, attenuation artifact) or from small-vessel disease. Finally and most importantly, the incongruence of CT angiography and myocardial perfusion imaging is inherent to the duality of morphologic versus functional testing (9,10). The technologic refinements implemented in the 64-section CT scanner generation have reduced the number of nonevaluable coronary segments (15,16), and further improvements may be expected with dual-source CT technology (8). However, the results of the present study and previous studies (15–17) support the notion that no matter how accurate CT angiography will possibly get with future technical advances, the two pieces of information obtained with myocardial perfusion imaging and morphology are difficult to compare. For example, our ROC analysis for the detection of perfusion defects showed similar AUCs for the reference standard, conventional angiography, and CT angiography, documenting a comparable performance of both techniques. Hence, many factors that are beyond the simple quantification of diameter narrowing and that therefore cannot be fully assessed with luminology will eventually determine whether or not a given lesion produces stress-induced ischemia. The calculated lesion severity cutoff value for predicting ischemia lies well within 50%–75%, which is generally perceived as the range of intermediate severity. A slightly lower cutoff value may be applied for patients with lower prevalence than that in our study population, as the high NPV of CT angiography renders this test most appropriate for ruling out CAD (15,16,18).

Our study results confirm good agreement between 64-section CT angiography and conventional coronary angiography for the diagnosis of coronary artery stenoses. Nonetheless, motion artifacts and extensive calcifications of the coronary arteries remain a major limitation for a reliable luminal interpretation, despite the above-mentioned technical developments, and conventional coronary angiography is often needed to verify the findings at CT angiography. On the other hand, CT angiography provides additional information on plaque morphology (eg, lipid-laden plaques, ulcerations) (32) that may be useful in guiding therapeutic decisions and affect long-term prognosis. It appears reasonable to hypothesize that patients with normal perfusion at presentation despite subclinical atherosclerosis might be at low short-term risk but high long-term risk for cardiac events (33). However, the potential clinical value of such information remains to be elucidated and was beyond the scope of the present study.

Our study had limitations. There are shortcomings to using SPECT as the reference standard for functional relevant coronary stenoses. SPECT has a high sensitivity in the detection of significant coronary stenoses, but its specificity is somewhat lower, as SPECT is susceptible to a variety of artifacts (photon attenuation, respiratory motion, spillover from gut or liver activity) (11). In addition, the tetrofosmin myocardial uptake curve plateaus at lower levels of hyperemia than thallium. Therefore, the use of vasodilator stress has been questioned by some authors (34), although no difference was found between the technetium-labeled tracers and thallium in a large randomized multicenter trial (35). Considering the large experience accumulated over 2 decades, including the prognostic information of SPECT myocardial perfusion imaging, this technique can be regarded as being the best-evaluated and -established noninvasive imaging tool for the hemodynamic assessment of CAD. Moreover, the use of x-ray–based attenuation correction and information from gated SPECT—as in our patients—is known to improve the specificity of SPECT myocardial perfusion imaging studies without affecting their sensitivity (11). Regarding CT angiography, to reduce radiation exposure in our study, prospective tube current modulation was used in all patients. This technique allows a reduction in radiation exposure of up to 50% but may preclude the use of early systolic to midsystolic phases for coronary reconstruction at higher heart rates or in cases of arrhythmia.

In summary, 64-section CT angiography is a reliable tool for identifying patients without hemodynamically relevant CAD in an intermediate-to-high–risk population. Its implementation in clinical practice may help avoid the expense and high resource utilization incumbent with catheterization laboratory studies. Our results suggest that a multicenter trial, required to confirm these data, is justified. On the other hand, an abnormal CT angiography study—like an abnormal conventional angiography study—is a poor predictor of ischemia. Conversely, a normal myocardial perfusion imaging study does not exclude the presence of subclinical CAD as assessed with CT and conventional angiography for which aggressive cardiovascular risk modification may be warranted. This underlines the potential value of a comprehensive noninvasive CAD assessment including both morphologic and hemodynamic information.

Acknowledgment: We are grateful to our Deputy Chief Radiographer, Ratko Milovanovic, for his excellent technical support.

References

1. Hendel RC, Patel MR, Kramer CM, et al. ACCF/ACR/SCCT/SCMR/ASNC/NASCI/SCAI/SIR 2006 appropriateness criteria for cardiac computed tomography and cardiac magnetic resonance imaging: a report of the American College of Cardiology Foundation Quality Strategic Directions Committee Appropriateness Criteria Working Group, American College of Radiology, Society of Cardiovascular Computed Tomography, Society for Cardiovascular Magnetic Resonance, American Society of Nuclear Cardiology, North American Society for Cardiac Imaging, Society for Cardiovascular Angiography and Interventions, and Society of Interventional Radiology. J Am Coll Cardiol 2006;48:1475–1497.

2. Budoff MJ, Achenbach S, Blumenthal RS, et al. Assessment of coronary artery disease by cardiac computed tomography: a scientific statement from the American Heart Association Committee on Cardiovascular Imaging and Intervention, Council on Cardiovascular Radiology and Intervention, and Committee on Cardiac Imaging, Council on Clinical Cardiology. Circulation 2006;114:1761–1791.

3. Raff GL, Gallagher MJ, O'Neill WW, Goldstein JA. Diagnostic accuracy of noninvasive coronary angiography using 64-slice

spiral computed tomography. J Am Coll Cardiol 2005;46:552–557.

4. Pugliese F, Mollet NR, Runza G, et al. Diagnostic accuracy of non-invasive 64-slice CT coronary angiography in patients with stable angina pectoris. Eur Radiol 2006;16:575–582.
5. Mollet NR, Cademartiri F, van Mieghem CA, et al. High-resolution spiral computed tomography coronary angiography in patients referred for diagnostic conventional coronary angiography. Circulation 2005;112:2318–2323.
6. Leschka S, Alkadhi H, Plass A, et al. Accuracy of MSCT coronary angiography with 64-slice technology: first experience. Eur Heart J 2005;26:1482–1487.
7. Leber AW, Knez A, von Ziegler F, et al. Quantification of obstructive and nonobstructive coronary lesions by 64-slice computed tomography: a comparative study with quantitative coronary angiography and intravascular ultrasound. J Am Coll Cardiol 2005;46:147–154.
8. Scheffel H, Alkadhi H, Plass A, et al. Accuracy of dual-source CT coronary angiography: first experience in a high pre-test probability population without heart rate control. Eur Radiol 2006;16:2739–2747.
9. Topol EJ, Nissen SE. Our preoccupation with coronary luminology: the dissociation between clinical and angiographic findings in ischemic heart disease. Circulation 1995;92:2333–2342.
10. White CW, Wright CB, Doty DB, et al. Does visual interpretation of the coronary arteriogram predict the physiologic importance of a coronary stenosis? N Engl J Med 1984;310:819–824.
11. Klocke FJ, Baird MG, Lorell BH, et al. ACC/AHA/ASNC guidelines for the clinical use of cardiac radionuclide imaging: executive summary—a report of the American College of Cardiology/American Heart Association Task Force on Practice Guidelines (ACC/AHA/ASNC Committee to Revise the 1995 Guidelines for the Clinical Use of Cardiac Radionuclide Imaging). J Am Coll Cardiol 2003;42:1318–1333.
12. Iskander S, Iskandrian AE. Risk assessment using single-photon emission computed tomographic technetium-99m sestamibi imaging. J Am Coll Cardiol 1998;32:57–62.
13. Hachamovitch R, Berman DS, Shaw LJ, et al. Incremental prognostic value of myocardial perfusion single photon emission computed tomography for the prediction of cardiac death: differential stratification for risk of cardiac death and myocardial infarction. Circulation 1998;97:535–543.
14. Hachamovitch R, Hayes SW, Friedman JD, Cohen I, Berman DS. Comparison of the short-term survival benefit associated with revascularization compared with medical therapy in patients with no prior coronary artery disease undergoing stress myocardial perfusion single photon emission computed tomography. Circulation 2003;107:2900–2907.
15. Hacker M, Jakobs T, Matthiesen F, et al. Comparison of spiral multidetector CT angiography and myocardial perfusion imaging in the noninvasive detection of functionally relevant coronary artery lesions: first clinical experiences. J Nucl Med 2005;46:1294–1300.
16. Hacker M, Jakobs T, Hack N, et al. Sixty-four slice spiral CT angiography does not predict the functional relevance of coronary artery stenoses in patients with stable angina. Eur J Nucl Med Mol Imaging 2006;34:4–10.
17. Schuijf JD, Wijns W, Jukema JW, et al. Relationship between noninvasive coronary angiography with multi-slice computed tomography and myocardial perfusion imaging. J Am Coll Cardiol 2006;48:2508–2514.
18. Gaemperli O, Schepis T, Koepfli P, et al. Accuracy of 64-slice CT angiography for the detection of functionally relevant coronary stenoses as assessed with myocardial perfusion SPECT. Eur J Nucl Med Mol Imaging 2007;34:1162–1171.
19. Bossuyt PM, Reitsma JB, Bruns DE, et al. Towards complete and accurate reporting of studies of diagnostic accuracy: the STARD initiative. Radiology 2003;226:24–28.
20. Leschka S, Wildermuth S, Boehm T, et al. Noninvasive coronary angiography with 64-section CT: effect of average heart rate and heart rate variability on image quality. Radiology 2006;241:378–385.
21. Austen WG, Edwards JE, Frye RL, et al. A reporting system on patients evaluated for coronary artery disease. Report of the Ad Hoc Committee for Grading of Coronary Artery Disease, Council on Cardiovascular Surgery, American Heart Association. Circulation 1975;51:5–40.
22. Cerqueira MD, Verani MS, Schwaiger M, Heo J, Iskandrian AS. Safety profile of adenosine stress perfusion imaging: results from the Adenoscan Multicenter Trial Registry. J Am Coll Cardiol 1994;23:384–389.
23. Hesse B, Tagil K, Cuocolo A, et al. EANM/ESC procedural guidelines for myocardial perfusion imaging in nuclear cardiology. Eur J Nucl Med Mol Imaging 2005;32:855–897.
24. Koepfli P, Hany TF, Wyss CA, et al. CT attenuation correction for myocardial perfusion quantification using a PET/CT hybrid scanner. J Nucl Med 2004;45:537–542.
25. Fricke H, Fricke E, Weise R, Kammeier A, Lindner O, Burchert W. A method to remove artifacts in attenuation-corrected myocardial perfusion SPECT introduced by misalignment between emission scan and CT-derived attenuation maps. J Nucl Med 2004;45:1619–1625.
26. Germano G, Kavanagh PB, Waechter P, et al. A new algorithm for the quantitation of myocardial perfusion SPECT. I. Technical principles and reproducibility. J Nucl Med 2000;41:712–719.
27. Fleischmann S, Koepfli P, Namdar M, Wyss CA, Jenni R, Kaufmann PA. Gated (99m)Tc-tetrofosmin SPECT for discriminating infarct from artifact in fixed myocardial perfusion defects. J Nucl Med 2004;45:754–759.
28. Obuchowski NA. Receiver operating characteristic curves and their use in radiology. Radiology 2003;229:3–8.
29. Garcia MJ, Lessick J, Hoffmann MH. Accuracy of 16-row multidetector computed tomography for the assessment of coronary artery stenosis. JAMA 2006;296:403–411.
30. Altman DG, Bland JM. Diagnostic tests 2: predictive values. BMJ 1994;309:102.
31. Fluss R, Faraggi D, Reiser B. Estimation of the Youden Index and its associated cutoff point. Biom J 2005;47:458–472.
32. Hausleiter J, Meyer T, Hadamitzky M, Kastrati A, Martinoff S, Schomig A. Prevalence of noncalcified coronary plaques by 64-slice computed tomography in patients with an intermediate risk for significant coronary artery disease. J Am Coll Cardiol 2006;48:312–318.
33. Berman DS, Hachamovitch R, Shaw LJ, et al. Roles of nuclear cardiology, cardiac computed tomography, and cardiac magnetic resonance: noninvasive risk stratification and a conceptual framework for the selection of noninvasive imaging tests in patients with known or suspected coronary artery disease. J Nucl Med 2006;47:1107–1118.
34. Glover DK, Ruiz M, Yang JY, Smith WH, Watson DD, Beller GA. Myocardial 99mTc-tetrofosmin uptake during adenosine-induced vasodilatation with either a critical or mild coronary stenosis: comparison with 201Tl and regional myocardial blood flow. Circulation 1997;96:2332–2338.
35. Kapur A, Latus KA, Davies G, et al. A comparison of three radionuclide myocardial perfusion tracers in clinical practice: the ROBUST study. Eur J Nucl Med Mol Imaging 2002;29:1608–1616.

Radiology 2008

This is your reprint order form or pro forma invoice

(Please keep a copy of this document for your records.)

Reprint order forms and purchase orders or prepayments must be received 72 hours after receipt of form either by mail or by fax at 410-820-9765. It is the policy of Cadmus Reprints to issue one invoice per order. **Please print clearly**.

Author Name _____
Title of Article _____
Issue of Journal_____ Reprint # _____ Publication Date _____
Number of Pages_____ KB # _____ Symbol Radiology
Color in Article? Yes / No (Please Circle)

Please include the journal name and reprint number or manuscript number on your purchase order or other correspondence.

Order and Shipping Information

Reprint Costs (Please see page 2 of 2 for reprint costs/fees.)

_____ Number of reprints ordered $_____
_____ Number of color reprints ordered $_____
_____ Number of covers ordered $_____
Subtotal $_____
Taxes $_____

(*Add appropriate sales tax for Virginia, Maryland, Pennsylvania, and the District of Columbia or Canadian GST to the reprints if your order is to be shipped to these locations*.)

First address included, add $32 for each additional shipping address $_____

TOTAL $_____

Shipping Address (cannot ship to a P.O. Box) Please Print Clearly

Name _____
Institution _____
Street _____
City _____ State _____ Zip _____
Country _____
Quantity_____ Fax _____
Phone: Day _____ Evening _____
E-mail Address _____

Additional Shipping Address* (cannot ship to a P.O. Box)

Name _____
Institution _____
Street _____
City _____ State _____ Zip _____
Country _____
Quantity _____ Fax _____
Phone: Day _____ Evening _____
E-mail Address _____
** Add $32 for each additional shipping address*

Payment and Credit Card Details

Enclosed: Personal Check _____
Credit Card Payment Details _____
Checks must be paid in U.S. dollars and drawn on a U.S. Bank.

Credit Card: __ VISA __ Am. Exp. __ MasterCard
Card Number _____
Expiration Date_____
Signature: _____

Please send your order form and prepayment made payable to:

Cadmus Reprints
P.O. Box 751903
Charlotte, NC 28275-1903

Note: Do not send express packages to this location, PO Box.
FEIN #:541274108

Invoice or Credit Card Information

Invoice Address Please Print Clearly
Please complete Invoice address as it appears on credit card statement

Name _____
Institution _____
Department _____
Street _____
City _____ State _____ Zip _____
Country _____
Phone _____ Fax _____
E-mail Address _____

Cadmus will process credit cards and *Cadmus Journal Services* will appear on the credit card statement.

If you don't mail your order form, you may fax it to 410-820-9765 with your credit card information.

Signature _____ Date _____

Signature is required. By signing this form, the author agrees to accept the responsibility for the payment of reprints and/or all charges described in this document.

RB-9/26/07

Radiology 2008

Black and White Reprint Prices

Domestic (USA only)						
# of Pages	50	100	200	300	400	500
1-4	$221	$233	$268	$285	$303	$323
5-8	$355	$382	$432	$466	$510	$544
9-12	$466	$513	$595	$652	$714	$775
13-16	$576	$640	$749	$830	$912	$995
17-20	$694	$775	$906	$1,017	$1,117	$1,220
21-24	$809	$906	$1,071	$1,200	$1,321	$1,471
25-28	$928	$1,041	$1,242	$1,390	$1,544	$1,688
29-32	$1,042	$1,178	$1,403	$1,568	$1,751	$1,924
Covers	$97	$118	$215	$323	$442	$555

International (includes Canada and Mexico)						
# of Pages	50	100	200	300	400	500
1-4	$272	$283	$340	$397	$446	$506
5-8	$428	$455	$576	$675	$784	$884
9-12	$580	$626	$805	$964	$1,115	$1,278
13-16	$724	$786	$1,023	$1,232	$1,445	$1,652
17-20	$878	$958	$1,246	$1,520	$1,774	$2,030
21-24	$1,022	$1,119	$1,474	$1,795	$2,108	$2,426
25-28	$1,176	$1,291	$1,700	$2,070	$2,450	$2,813
29-32	$1,316	$1,452	$1,936	$2,355	$2,784	$3,209
Covers	$156	$176	$335	$525	$716	$905

Minimum order is 50 copies. For orders larger than 500 copies, please consult Cadmus Reprints at 800-407-9190.

Reprint Cover

Cover prices are listed above. The cover will include the publication title, article title, and author name in black.

Shipping

Shipping costs are included in the reprint prices. Domestic orders are shipped via UPS Ground service. Foreign orders are shipped via a proof of delivery air service.

Multiple Shipments

Orders can be shipped to more than one location. Please be aware that it will cost $32 for each additional location.

Delivery

Your order will be shipped within 2 weeks of the journal print date. Allow extra time for delivery.

Color Reprint Prices

Domestic (USA only)						
# of Pages	50	100	200	300	400	500
1-4	$223	$239	$352	$473	$597	$719
5-8	$349	$401	$601	$849	$1,099	$1,349
9-12	$486	$517	$852	$1,232	$1,609	$1,992
13-16	$615	$651	$1,105	$1,609	$2,117	$2,624
17-20	$759	$787	$1,357	$1,997	$2,626	$3,260
21-24	$897	$924	$1,611	$2,376	$3,135	$3,905
25-28	$1,033	$1,071	$1,873	$2,757	$3,650	$4,536
29-32	$1,175	$1,208	$2,122	$3,138	$4,162	$5,180
Covers	$97	$118	$215	$323	$442	$555

International (includes Canada and Mexico))						
# of Pages	50	100	200	300	400	500
1-4	$278	$290	$424	$586	$741	$904
5-8	$429	$472	$746	$1,058	$1,374	$1,690
9-12	$604	$629	$1,061	$1,545	$2,011	$2,494
13-16	$766	$797	$1,378	$2,013	$2,647	$3,280
17-20	$945	$972	$1,698	$2,499	$3,282	$4,069
21-24	$1,110	$1,139	$2,015	$2,970	$3,921	$4,873
25-28	$1,290	$1,321	$2,333	$3,437	$4,556	$5,661
29-32	$1,455	$1,482	$2,652	$3,924	$5,193	$6,462
Covers	$156	$176	$335	$525	$716	$905

Tax Due

Residents of Virginia, Maryland, Pennsylvania, and the District of Columbia are required to add the appropriate sales tax to each reprint order. For orders shipped to Canada, please add 7% Canadian GST unless exemption is claimed.

Ordering

Reprint order forms and purchase order or prepayment is required to process your order. Please reference journal name and reprint number or manuscript number on any correspondence. You may use the reverse side of this form as a proforma invoice. Please return your order form and prepayment to:

Cadmus Reprints
P.O. Box 751903
Charlotte, NC 28275-1903

Note: Do not send express packages to this location, PO Box.
FEIN #:541274108

Please direct all inquiries to:

Rose A. Baynard
800-407-9190 (toll free number)
410-819-3966 (direct number)
410-820-9765 (FAX number)
baynardr@cadmus.com (e-mail)

Reprint Order Forms and purchase order or prepayments must be received 72 hours after receipt of form.